

archives
of thermodynamics
Vol. **31**(2010), No. 1, 33-43
DOI: 10.2478/v10173-010-0002-0

Numerical modeling of heat and mass transfer in cylindrical ducts

PIOTR DUDA*
GRZEGORZ MAZURKIEWICZ

Cracow University of Technology, Institute of Process and Power Engineering,
Al. Jana Pawła II 37, 31-864 Kraków

Abstract In this work, numerical modeling of steady state heat and mass transfer is presented. Both laminar and hydrodynamically fully developed turbulent flow in a pipe are shown. Numerical results are compared with values obtained from analytical solution of such problems. The problems under consideration are often denoted as extended Graetz problems. They occur in heat exchangers using liquid metals as working fluid, in cooling systems for electric components or in chemical process lines. Calculations were carried out gradually decreasing the mesh size in order to examine the convergence of numerical method to analytical solution.

Keywords: Graetz problem; Numerical solution; Heat transfer; Laminar and turbulent flow

Nomenclature

c	–	specific heat, J/(kg K)
d	–	diameter of cylindrical duct, m
f_μ	–	constant of proportionality
L	–	characteristic dimension, m
L_t	–	characteristic scale of velocity, m
Pe	–	Peclet number
Pr	–	Prandtl number
r	–	radius, m
\tilde{r}	–	dimensionless radius

*Corresponding author. E-mail address: pduda@mech.pk.edu.pl

R	–	radius of cylindrical duct, m
Re	–	Reynolds number
T	–	temperature, K
T_1	–	internal temperature of the surface of the cylindrical duct for $x < 0$, K
T_2	–	internal temperature of the surface of the cylindrical duct for $x > 0$, K
U_t	–	scale of the largest vortex, K
u	–	velocity in x dimension, m/s
\bar{u}	–	medium velocity in x direction, m/s
\tilde{u}	–	dimensionless velocity in x direction
v	–	velocity in r direction, m/s
V	–	volume of fluid, m ³
x	–	distance calculated along the axis of the duct, m
\tilde{x}	–	dimensionless distance calculated along the axis of the duct

Greek symbols

ε_{hr}	–	eddy diffusivity for heat transfer in r direction, m ² /s
ε_{hx}	–	eddy diffusivity for heat transfer in x direction, m ² /s
ε_m	–	eddy diffusivity for momentum transfer, m ² /s
$\tilde{\varepsilon}_m$	–	dimensionless eddy diffusivity for momentum transfer
η	–	dynamic viscosity, Pa s
Θ	–	dimensionless temperature
λ	–	heat conductivity, W/(m K)
μ_t	–	eddy viscosity, Pa s
ρ	–	density, kg/m ³

1 Extended Graetz problem

The geometry of a cylindrical duct and the applied coordinate system are presented in Fig. 1.

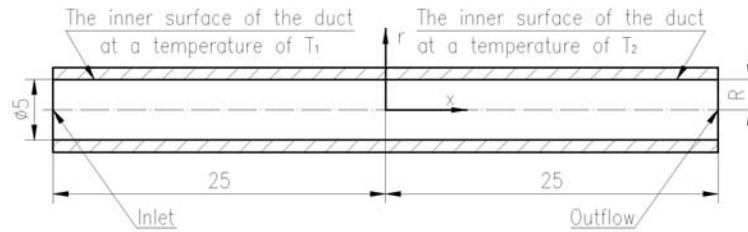


Figure 1. Geometry and coordinate system, mm.

The cylindrical duct was divided into two heating sections. The first one was extending for $x < 0$ with constant wall temperature T_1 and the second one for $x > 0$ with constant wall temperature T_2 , where $T_1 < T_2$. Moreover, it was assumed that fluid properties are constant and independent of tem-

perature, the Peclet number is low, the flow in duct is hydrodynamically fully developed and the velocity profile is fully developed. This means that the vertical velocity component v is zero and axial velocity component is only a function of the coordinate orthogonal to the main flow direction [1].

Assumptions above allow formulating the energy equations [2], which reads:

$$\rho c u(r) \frac{\partial T}{\partial x} = \frac{1}{r} \frac{\partial}{\partial r} \left[r \left(\lambda \frac{\partial T}{\partial r} - \rho c \overline{v'T'} \right) \right] + \frac{\partial}{\partial x} \left[\lambda \frac{\partial T}{\partial x} - \rho c \overline{u'T'} \right]. \quad (1)$$

If one analyses Eq. (1) for laminar flow ($\overline{v'T'} = 0$, $\overline{u'T'} = 0$), one finds immediately that the equation is elliptic in nature. This is due to the axial heat conduction effect within the flow, which is represented by the second term on the right hand side of the equation. For turbulent flow, the nature of the equation will also depend on turbulent heat fluxes. The turbulent heat fluxes $-\rho c \overline{v'T'}$ and $-\rho c \overline{u'T'}$ have to be modeled. This can be done by using a simple eddy viscosity model [1] Eq. (2).

$$-\overline{v'T'} = \varepsilon_{hr} \frac{\partial T}{\partial r}, \quad -\overline{u'T'} = \varepsilon_{hx} \frac{\partial T}{\partial x}, \quad (2)$$

where ε_{hr} and ε_{hx} are only functions of the coordinate orthogonal to the flow direction.

If one introduces the following dimensionless quantities into above equations

$$\Theta = \frac{T - T_2}{T_1 - T_2}, \quad \tilde{r} = \frac{r}{R}, \quad \tilde{x} = \frac{x}{R} \frac{1}{\text{Re} \cdot \text{Pr}}, \quad \text{Pr} = \frac{\eta c}{\lambda}, \quad (3)$$

$$\text{Re} = \frac{\rho R \bar{u}}{\eta}, \quad \tilde{\varepsilon}_m = \frac{\varepsilon_m \rho}{\eta}, \quad \tilde{u} = \frac{u}{\bar{u}}, \quad \text{Pe} = \text{Re} \text{Pr},$$

the energy equation is given

$$\tilde{u}(\tilde{r}) \frac{\partial \Theta}{\partial \tilde{x}} = \frac{1}{\text{Pe}^2} \frac{\partial}{\partial \tilde{x}} \left[a_1(\tilde{r}) \frac{\partial \Theta}{\partial \tilde{x}} \right] + \frac{1}{\tilde{r}} \frac{\partial}{\partial \tilde{r}} \left[\tilde{r} a_2(\tilde{r}) \frac{\partial \Theta}{\partial \tilde{r}} \right]. \quad (4)$$

Where the functions $a_1(\tilde{r})$ and $a_2(\tilde{r})$ are described by relations:

$$a_1(\tilde{r}) = 1 + \frac{\text{Pr}}{\text{Pr}_t} \tilde{\varepsilon}_m, \quad a_2(\tilde{r}) = 1 + \frac{\text{Pr}}{\text{Pr}_t} \left(\frac{\varepsilon_{hx}}{\varepsilon_{hr}} \right) \tilde{\varepsilon}_m, \quad \text{Pr}_t = \frac{\tilde{\varepsilon}_m}{\tilde{\varepsilon}_{hr}}. \quad (5)$$

The boundary conditions for Eq. (4) read

$$\begin{aligned}
 \tilde{r} = 1 : \Theta = 0, \quad \tilde{x} \leq 0 \\
 \Theta = 1, \quad \tilde{x} > 0 \\
 \tilde{r} = 0 : \frac{\partial \Theta}{\partial \tilde{r}} = 0 \\
 \lim_{\tilde{x} \rightarrow -\infty} \Theta = 0, \quad \lim_{\tilde{x} \rightarrow +\infty} \Theta = 1
 \end{aligned} \quad (6)$$

Above equations are form a complete set of equations necessary to solve the analytically extended Graetz problem.

2 Cylindrical duct

ANSYS ICEM CFD software was used to generate the geometry of a cylindrical duct and finite volume grid. Mesh A, B and C were generated. Generation of completely regular grid in the entire volume of the fluid is not possible because of its shape. To minimize numerical errors the fluid's boundary layer was generated, which has a great influence on heat transfer between the cylindrical duct and fluid.

Fig. 2a, b and c present cross-section of the fluid domain divided into finite volume mesh. In the main fluid flow direction the pipe was divided into 62 nodes for mesh A, 125 nodes for mesh B and 500 nodes for mesh C for laminar flow. For turbulent flow the pipe generating line was divided into 250 nodes for mesh A, 500 nodes for mesh B and for 1000 nodes for mesh C.

3 Numerical solution of the extended Graetz problem for laminar flow

The calculation of temperature distribution has been carried out using Ansys CFX software based on the finite volume method [3] and is presented in Fig. 3.

Helium at temperature of 500 K was assumed as fluid for the laminar flow, which has the following physical properties: density $\rho = 0.0976 \text{ kg/m}^3$, dynamic viscosity $\eta = 2.83 \cdot 10^{-5} \text{ Pa s}$, thermal conductivity $\lambda = 0.221 \text{ W/(m K)}$ and specific heat $c = 5197 \text{ J/(kg K)}$ [4]. In addition, the flow velocity at the inlet was equal to 0.875 m/s. For these parameters the Peclet number is close to 10,

$$Pe = 9.84 \approx 10. \quad (7)$$

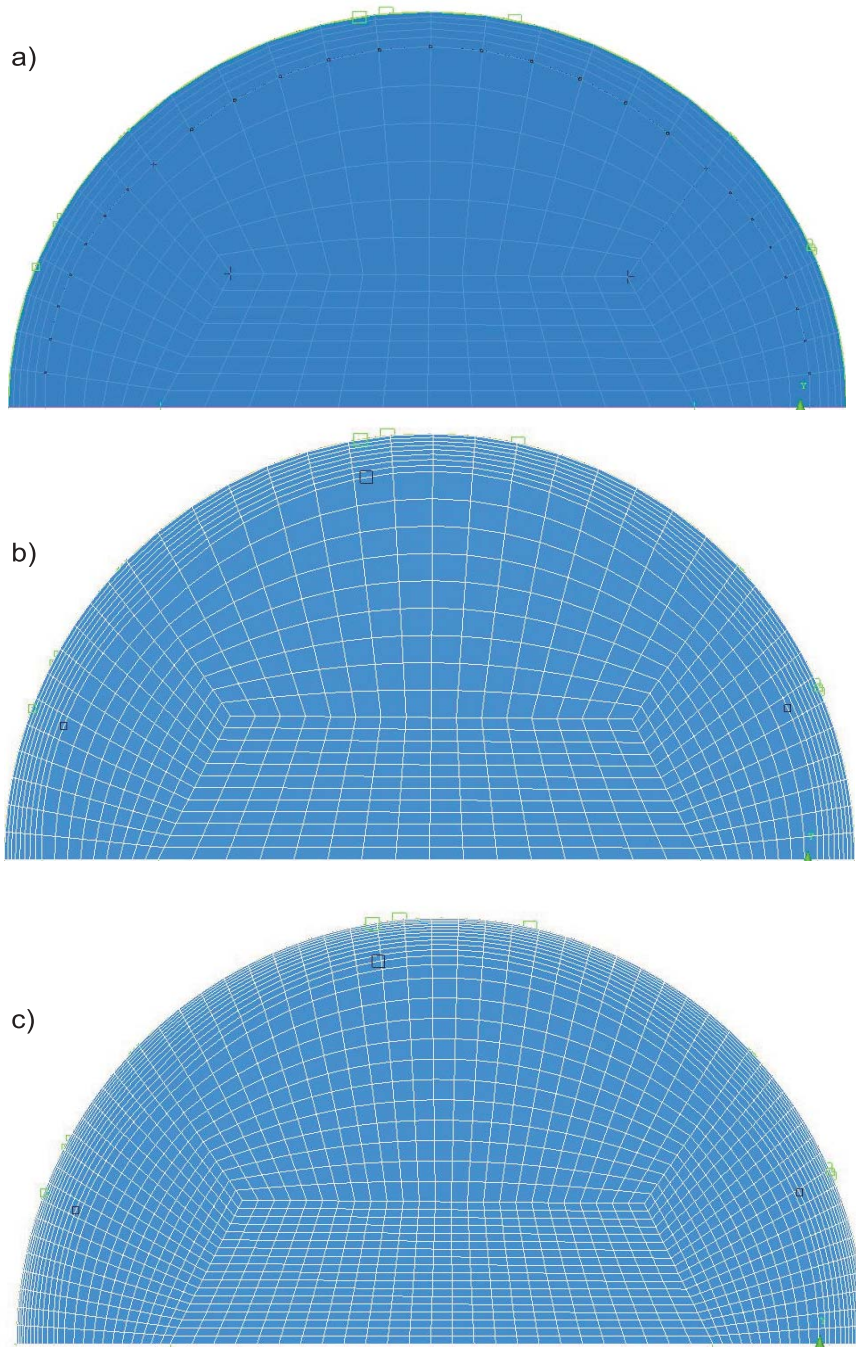


Figure 2. Mesh of the fluid domain: a) – mesh A, b) – mesh B, c) – mesh C.

According to the description in Sec. 1 the constant wall temperature boundary condition was assumed on inner surface of circular duct. The wall temperature was equal to $T_1 = 400$ K for the first heating section and for the second heating section $T_2 = 600$ K, respectively.

The calculated temperature distribution using the mesh C is shown in Fig. 3.

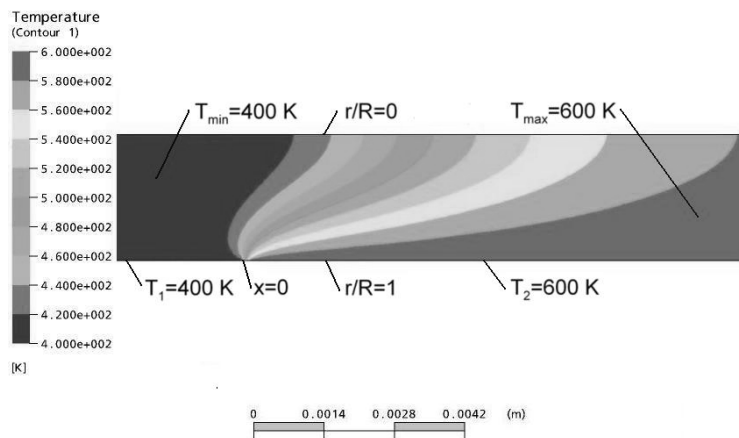


Figure 3. Temperature distribution in fluid for laminar flow using the mesh C, K.

In order to show the accuracy of numerical method the temperature distribution along the radius \tilde{r} in the dimensionless coordinates for twelve selected distances \tilde{x} from coordinate $\tilde{x} = 0$ for both numerical and analytical solutions is presented in Fig. 4a, b and c. Dimensionless temperature θ is placed on the ordinate axis and the dimensionless radius $\tilde{r} = r/R$, at which the temperature was determined, is located on the abscissa axis.

Table 1. Dimensionless and corresponding to them absolute distances from the point of abrupt temperature change ($\tilde{x} = 0$) for laminar flow.

Dimensionless distance	0.5	0.3	0.15	0.08	0.05	0.02	0.01	0.006	-0.008	-0.015	-0.02	-0.03
Absolute distance in [mm]	12.5	7.5	3.75	2	1.25	0.5	0.25	0.15	-0.2	-0.375	-0.5	-0.75

Distances from the point of abrupt temperature change ($\tilde{x} = 0$) were calculated according to relationship (3) and are shown in Tab. 1.

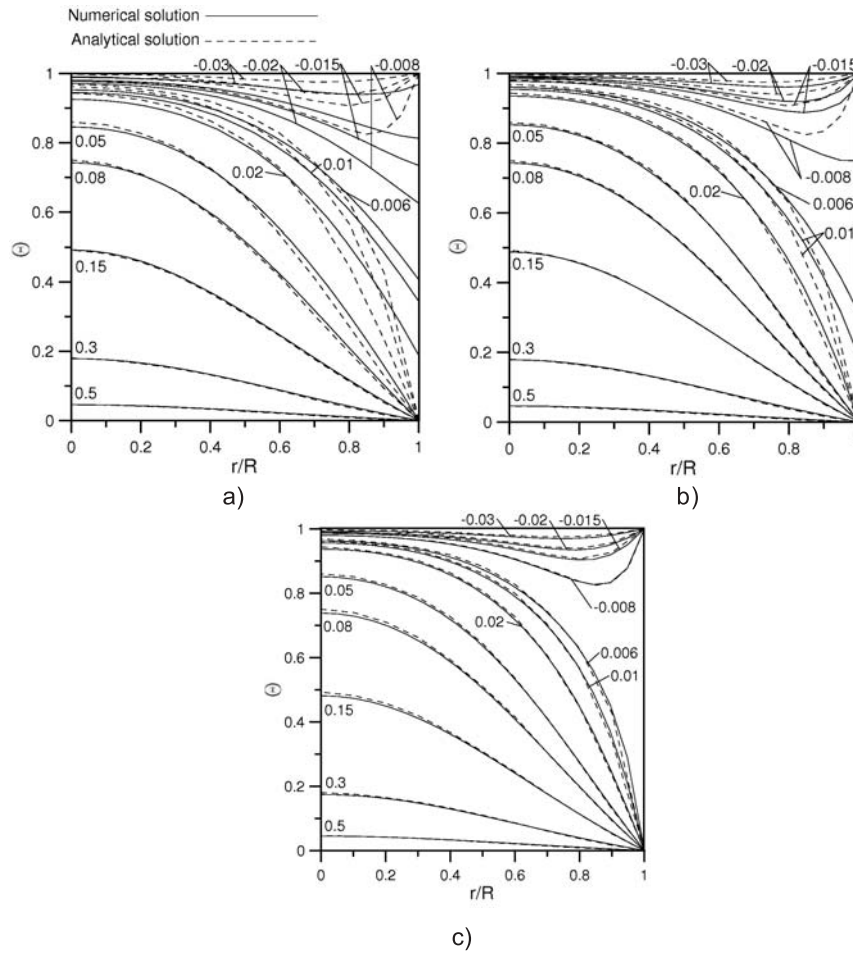


Figure 4. Comparison of temperature distribution obtained from numerical solution and from analytical solution for laminar flow: a) – mesh A, b) – mesh B, c) – mesh C.

By reducing the size of the mesh a better compatibility of the calculated results with the analytical solution is obtained. This is particularly well seen on the outer surface of the fluid ($r/R = 1$) and at the point of abrupt change of temperature ($x = 0$). Increasing the number of finite volumes one extends the time of calculations and increases the hardware requirements, so after obtaining the results that are accepted as satisfactory it is not indicated to reduce the size of the mesh again.

4 Numerical solution of the extended Graetz problem for turbulent flow

In the present work, zero equation model was used for both analytical and numerical solutions of turbulent flow.

In the zero equation model, turbulent viscosity is constant throughout the volume of fluid and is calculated on the basis of a characteristic velocity scale L_t and the scale of largest vortex U_t using empirical equation (8) [5, 6]. The main advantage of zero equation model is that it does not need to solve any additional equations of heat and mass transfer, which allows to simplify calculations and reduce their time.

In Ansys CFX software, turbulent viscosity is determined in accordance with the Prandtl model and Kolmogorov relationship:

$$\mu_t = \rho \cdot f_\mu \cdot U_t \cdot L_t, \quad (8)$$

where f_μ is a constant of proportionality, U_t designates as the highest speed in the observed volume and L_t have to be determined from relation:

$$L_t = \frac{V^{\frac{1}{3}}}{7}, \quad (9)$$

where V is the volume of fluid.

The working fluid properties were similar to mercury at the temperature of 873.15 K in order to have Prandtl number $Pr = 0.002$. In addition, the flow conditions were selected such that the corresponding Reynolds number was equal to $Re = 5000$. The following physical properties of fluid were assumed: density $\rho = 12816 \text{ kg/m}^3$, dynamic viscosity $\eta = 8.36 \cdot 10^{-4} \text{ Pa s}$, thermal conductivity $\lambda = 28 \text{ W/(m K)}$ and specific heat $c = 67 \text{ J/(kgK)}$ [3]. In addition, the flow velocity was equal to $v = 0.857 \text{ m/s}$.

According to Sec. 1 the constant wall temperature was assumed on the inner surface of circular duct. The wall temperature was equal to the value of $T_1 = 773.15 \text{ K}$ for $x < 0$ and $T_2 = 973.15 \text{ K}$ for $x > 0$. Temperature distribution has been calculated using Ansys CFX software based on the finite volume method and is presented for mesh C in Fig. 5.

In order to compare the obtained results with the analytical solution, numerical results have been transformed to the dimensionless coordinates:

$$\tilde{x} = \frac{x}{R} \cdot \frac{2}{Pe}. \quad (10)$$

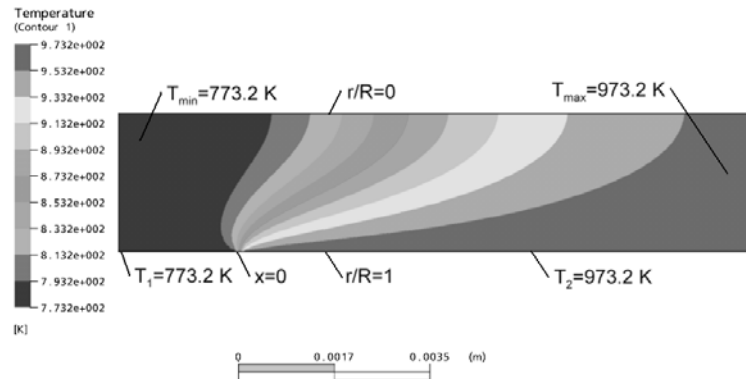


Figure 5. Temperature distribution in fluid for turbulent flow and mesh C, K.

They are shown in Fig. 6a, b and c for the mesh A, B and C using the turbulent viscosity 0.019 Pa s. Table 2 shows the dimensionless distance between the point $\tilde{x} = 0$ and the point where temperature was calculated together with corresponding absolute distance.

Table 2. Dimensionless and corresponding to them absolute distances from the point of abrupt temperature change ($\tilde{x} = 0$) for turbulent flow.

Dimensionless distance	0.3	0.15	0.08	0.05	0.012	0.004	-0.004	-0.006	-0.01	-0.02	-0.03	-0.05
Absolute distance in [mm]	3.75	1.875	1	0.625	0.15	0.05	-0.05	-0.075	-0.125	-0.25	-0.375	-0.625

Because the creation of an infinite pipe is impossible, the conditions of numerical calculations were not identical as in the model used in the analytical solution. To minimize the influence of the duct's length on the obtained results, calculations were performed for different turbulence viscosities. The best results were obtained when the turbulent viscosity was equal to 0.045 Pa s and are presented in Fig. 7.

Figure 6 presents the results of numerical calculations obtained for the mesh A, B and C and for the value of turbulent viscosity equal to 0.019 Pa s, which was assumed by ANSYS CFX software as a default (the turbulent viscosity determined by the length of the cylindrical duct).

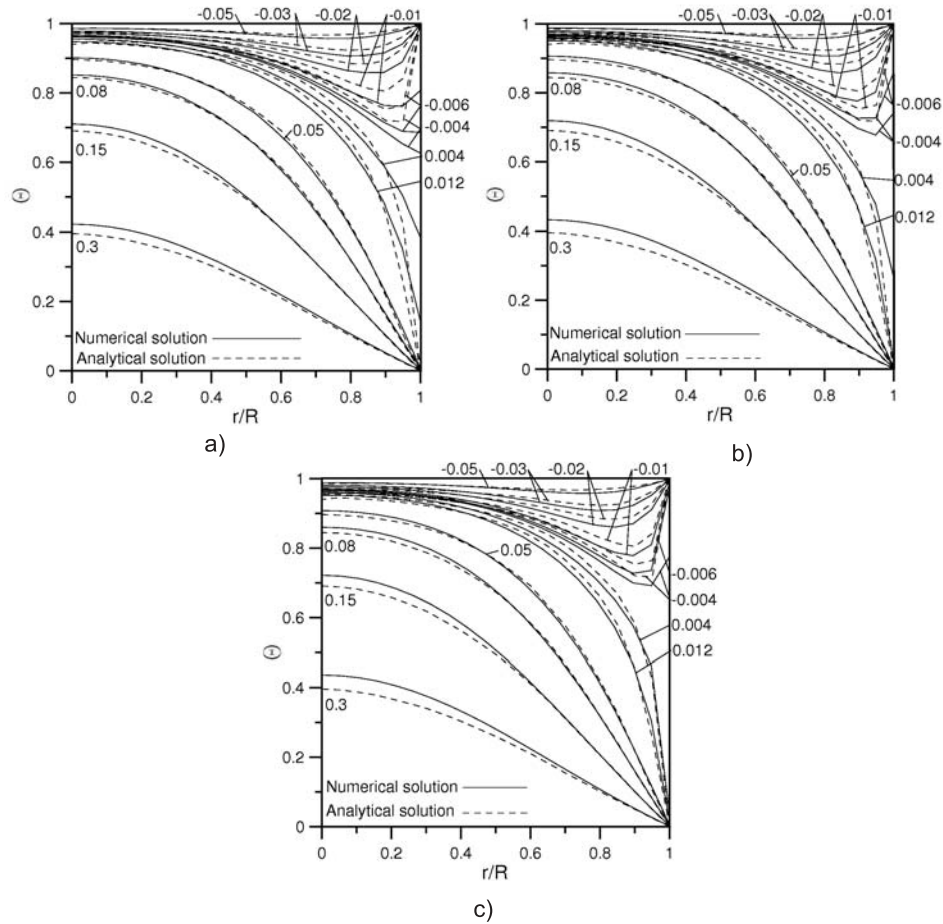


Figure 6. Comparison of temperature distribution obtained from numerical solution and from analytical solution for turbulent flow, zero equation model and eddy viscosity equal to 0.019 Pa s: a) – mesh A, b) – mesh B, c) – mesh C.

5 Conclusions

Numerical solution of the extended Graetz problem was presented for both laminar and turbulent flow.

The convergence of numerical solutions to the analytical ones with a decrease in the size of the mesh, was confirmed.

It was observed that the good compatibility of numerical calculations with the analytical solution was obtained if the mesh size in the direction

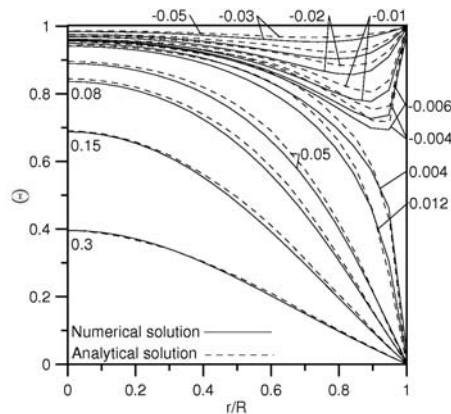


Figure 7. Comparison of results between numerical calculations and analytical solution for turbulent flow, zero equation model, eddy viscosity equal to 0.045 Pa s mesh C.

of the x -axis located at $x = 0$ was smaller than the first coordinate point at which the temperature was measured.

Received 16 July 2009

References

- [1] WEIGAND B.: *Analytical Methods for Heat Transfer and Fluid Flow Problems*, Springer-Verlag, Berlin Heidelberg 2006.
- [2] INCROPERA F DEWITT D. BERGMAN T. LAVINE A.: *Fundamentals of Heat and Mass Transfer*, Mechanical and Aerospace Engineering Department, University of California, Los Angeles 2005.
- [3] CENGEL Y. TURNER R.: *Fundamental of Thermal-Fluid Science*, New York 2001.
- [4] TALER J. DUDA P.: *Solving direct and inverse heat conduction problems*, Springer-Verlag, Berlin Heidelberg 2006.
- [5] GRYBOŚ R.: *Fundamentals of Fluid Mechanics*, PWN, Warszawa 1989 (in Polish).
- [6] *Ansys User's Manual. Revision 5.0 A*.